FPCM-9 (2008)
The 9th International Conference on Flow Processes in Composite Materials
Montréal (Québec), Canada
8 ~ 10 July 2008

IDENTIFICATION OF PREFORM COMPRESSIBILITY BY INVERSE METHOD

T. Ouahbi [1, 3], C. H. Park [1], A. Saouab [1], P. Ouagne [1], J. Bréard [1], S. Chatel [2]

[1] *Laboratoire d'Ondes et Milieux Complexes (LOMC), FRE 3102 CNRS-Université du Havre, 25 rue Philippe Lebon, BP 540, 76058, Le Havre, France*
[2] *European Aeronautic Defence and Space – Corporate Research Center, 12 rue Pasteur, BP 76, 92150 Suresnes Cedex, France, Email: sylvain.chatel@eads.net*
[3] *Corresponding author's Email: tariq.ouahbi@univ-lehavre.fr*

SUMMARY: The identification of the transverse properties of fabrics is becoming an important topic, as the transverse flow is significant in advanced liquid composite molding processes such as resin film infusion, vacuum assisted resin transfer molding process and compression resin transfer molding process. However, it is not easy to characterize the transverse permeability and the compressibility of preform, since the fluid flow and the mechanical response of fabrics simultaneously occur in the transverse direction. Due to the strong hydro-mechanical coupling, hence, it has been a common approach to identify the transverse properties either under the simplified assumption (uniform resin pressure in the transverse direction) or under the ideal case where the closed form solution is known. In previous works, we developed a numerical code to simulate the resin film infusion process and an experimental device to for the measurement of transverse compressibility and permeability considering different compression conditions; either imposed force or imposed speed of compression. In this work, we characterize the material behaviors in the transverse direction by incorporating the material model into the full numerical simulation of an actual filling process. To identify the model coefficients, inverse method is applied with experimental measurements.

KEYWORDS: identification, compressibility, hydro-mechanical coupling, inverse method, Resin Film Infusion (RFI)

INTRODUCTION

Liquid composite moulding (LCM) processes such as RTM (Resin Transfer Moulding) process and VARTM (Vacuum Assisted Resin Transfer Moulding) process, are commonly used techniques for the manufacture of advanced composite structures. These processes offer several advantages over more traditional composite moulding processes including reduced solvent emissions, achieved by containing potentially hazardous gases (i.e., styrene) within a closed

mould. Part quality, process repeatability and production rates can also be increased due to the potential for automation. Several investigators have proposed resin flow models in the RFI process [1-4]. However, viscous liquid infusion simulations are usually performed without taking into account the preform deformations. Several approaches have been proposed to improve these models. Sommer and Mortensen [5] studied infiltration of initially dry deformable porous medium by a pressurized liquid, taking into account the influence of variations in permeability of the deformed porous medium. Ambrosi et al. [6] dealt with the problem of injection in an elastic porous preform and fluid-structure interaction. Lopatnikov et al. [7] suggested an analytical solution for one-dimensional flow in the planar direction and compaction in the thickness direction, to describe infusion of resin under vacuum in deformable fibrous porous media.

In most of related works, the fabric is supposed to be uniformly deformed in the direction of applied stress and the fibre volume fraction remains uniform in this direction while it is variable in the principal flow direction. However, the principal resin flow and fabric deformation occur in the same direction (i.e. the thickness of product), in the RFI process. As a consequence, the fabric is not uniformly deformed and the fibre volume fraction is not uniform either, in the direction of applied stress, during the resin flow in the RFI process. For a more precise description of this hydro-mechanical coupling in RFI process, Ouahbi et al. [8] proposed a numerical modelling taking into account the differential pressure and compaction stresses in the thickness direction and using the Terzaghi's Law (1) to couple the resin pressure and the mechanical stress imposed to the preform.

$$\sigma_{tot} = \sigma^{'} + P \tag{1}$$

where σ_{tot} is the total stress, $\sigma^{'}$ is the effective stress and P is the resin pressure.

The compressibility behaviour of a fibrous material when loaded is of great importance in many composite materials manufacturing processes, in particular the Liquid Composite Moulding processes. In some cases, for example, RTM and CRTM (Compression Resin Transfer Moulding), the response to compaction determines the required tooling forces; in others, for example, RFI and VARTM, it determines the precise part thickness during the manufacturing process. Compaction response also affects the compression phase of both imposed-force and imposed-displacement in CRTM process. In another hands, the hydro-mechanical coupling model developed in [8] is based on experimentally determined material properties. The compressibility as well as the permeability behaviour of the preform is key entry parameter for the modelling of the process.

There have been many studies into the response of a fibrous material to load [9-12]. The compressibility behaviour of the preform is most of the time modelled by empirical laws [13, 14] based on experimental observation. The model of Toll and Manson [14] based on a power law formulation is frequently used:

$$\sigma^{'} = cV_f{}^{d} \tag{1}$$

where V_f is the fibre volume fraction and c, d are materials parameter. The power index d typically takes a value in the range 3–19 [10], depending on the particular architecture of the

fibrous material. Merhi et al. [15] proposed a "physical" explanation based on the beam theory for the value of *d* in the case of randomly aligned fibre bundles mat. For other types of reinforcement, the *d* value is obtained from experimental compressibility curves. Cadinot [16] found *b* values situated in the range 5-8 for mats, and in the range 9-14 for more ordered reinforcements such as UD or satin weaves. Moreover, the value of *d* can be greatly affected by variation of the compression speed due to the viscoelastic response of the reinforcements in compression [17]. The model developed by Ouahbi et al. [8] predicts the evolution of the reinforcements thickness submitted to hydro-mechanical loads. The goal of this work is to determine the compressibility curve corresponding to a hydro-mechanical solicitation determined experimentally. To attain this objective the numerical hydro-mechanical coupling code [8] is used with an inverse method.

Experimental Procedures

A device to establish hydro-mechanical loadings under various injection conditions such as pressure control or flow rate control and various compaction conditions such as stress or displacement control was set up. A schematic diagram of the device is shown in Fig. 1.

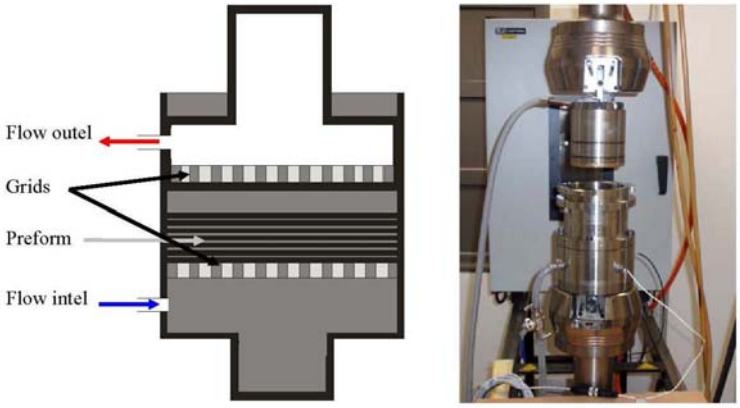

Fig. 1 Experimental device for Kz and compressibility measurement.

The fibrous reinforcement layers are placed between two perforated grids and a test fluid is injected at a constant flow rate. By the universal testing machine, the permeability evolution is determined by measuring the pressure difference before and after the fluid passage in the reinforcements as a function of the compression of the fibrous medium compression. The material used during this study is an E glass 5 harness satin weave. This material has an initial fibre volume fraction of ~ 48%. The thickness of an individual layer of fabric is 0.5mm. The fluid used in the experimental procedure is silicon oil of viscosity 0.1 Pa.s. Twenty layers of fabric are disposed for each test. The compaction velocity is ranged from 0.25 to 2 mm/min for the compressive test. Under stress condition, hydro-mechanical test are conducted following ramps of 5 kN/min and 10 kN/min up to a load of ~ 30 kN where the load is held constant to observe eventual viscoelastic recovery.

Hydromechanical Coupling under Imposed Stress

Under stress condition, the variation of thickness due to a constant mechanical stress rate is measured as a function of time. A fluid flow of constant flow rate is also applied to place the specimen of fabric under hydro-mechanical load. Fig. 2 shows the thickness variation of same preforms submitted to two different stress rates (5 and 10 kN/min) up to a load of 30 kN or a stress of 3.8 MPa.

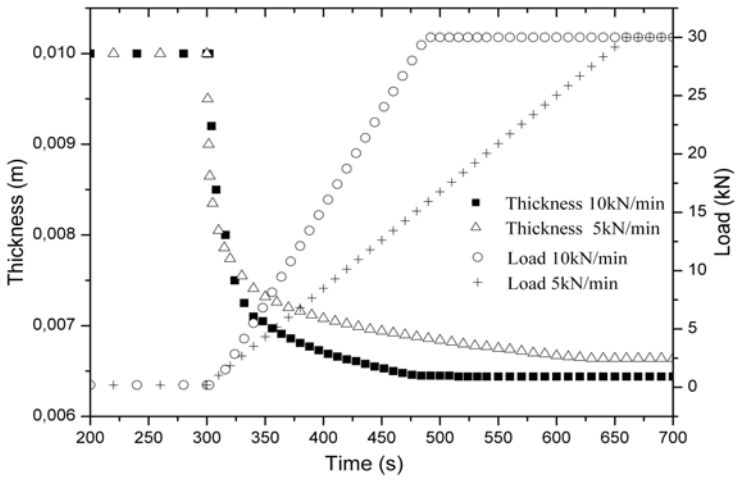

Fig. 2 Hydro-mechanical loading under different stress rates and flow rate conditions

When the ramp of mechanical stress is applied, the two curves show a fast decrease (with an average speed of 12 mm/min) in the reinforcement thickness over about 10 seconds. Between t = 310 s and t = 480 s for the 10kN/min curve and between t = 310 s and t = 660 s for the 5kN/min curve, the piston still submitted to the same stress rate and same constant flow. However, the value of the thickness of preforms does not reach a constant value. The final compression speed measured for the curve submitted to the 5 kN/min stress rate is about 0.1mm/min before the load reaches a value of 30 kN. The final compaction speed measured for the curve submitted to the 10 kN/min stress rate is about 0.15 mm/min. This demonstrates that during the compression at constant stress rate, the speed of compaction changes from about 12 to 0.1 mm/min. In terms of micro-mechanisms, the acceleration of the lower grid (between t ~ 300 and t ~310 s) with increasing applied stress is probably due to a quick fibre rearrangement and filling up of the porosity. Then rearrangement of the fibres becomes probably more and more difficult due to a higher level of fibre compression and lower porosity. Fig. 2 also shows that the final thickness of the samples submitted to 10 kN/min stress ramp is lower than the sample submitted to a 5 kN/min ramp. This confirms that the hydro-mechanical loading of a 5 harness satin glass weave exhibits a strong viscoelastic behaviour.

Identification of Preform Compressibility

An inverse method is implemented in the hydro-mechanical code [8] to establish the compressibility curves corresponding to the two hydro-mechanical curves shown in Figure 3.

Inverse Method

We present an inverse method to obtain the compressibility of the preform, by computing the two parameters *c* and *d* of the power's law of model of Toll and Manson [14]. In general, the parameters in a model are fitted by comparing the experimental data and the computational data. The deviation between the measured and the computational values is expressed by a least square form (3)

$$S(c,d)=\frac{1}{2}\sum_{i=1}^{N}\left[\frac{H_i^c(c,d)-H_i^m}{H_i^m}\right]^2 \tag{3}$$

where H_i^c and H_i^m are the computational and the measured thickness at the *i*th sensor locations. *N* is the number of sensors and *c*, *d* are the coefficients of the power law. The *c* and *d* coefficients can be obtained by minimizing the function defined in equation 3 and by finding the corresponding preform compressibility. The computed thicknesses are obtained repeatedly changing the compressibility values iteratively through the optimization procedure.

Gradient and Hessian Matrix

In general, the gradients and the Hessian matrix (the second derivative matrix) are required for a function minimization [18]. The gradients are defined by a next equation.

$$\beta_c=\frac{\partial S}{\partial c}=\sum_{i=1}^{N}\frac{H_i^c(c,d)-H_i^m}{\left(H_i^m\right)^2}\frac{\partial H_i^c(c,d)}{\partial c} \quad \text{and} \quad \beta_d=\frac{\partial S}{\partial d}=\sum_{i=1}^{N}\frac{H_i^c(c,d)-H_i^m}{\left(H_i^m\right)^2}\frac{\partial H_i^c(c,d)}{\partial d} \tag{4}$$

The Hessian matrix is associated with the second derivative of a given function to be minimized. It can be obtained by taking an additional partial derivative. It is usually defined by the following equation:

$$\alpha_{cd}=\frac{\partial^2 S}{\partial c\partial d}=\sum_{i=1}^{N}\frac{1}{\left(H_i^m\right)^2}\left[\frac{\partial H_i^c(c,d)}{\partial c}\frac{\partial H_i^c(c,d)}{\partial d}\right],$$

$$\alpha_{cc}=\frac{\partial^2 S}{\partial c\partial c}=\sum_{i=1}^{N}\frac{1}{\left(H_i^m\right)^2}\left[\frac{\partial H_i^c(c,d)}{\partial c}\right]^2 \quad \text{and} \quad \alpha_{dd}=\frac{\partial^2 S}{\partial d\partial d}=\sum_{i=1}^{N}\frac{1}{\left(H_i^m\right)^2}\left[\frac{\partial H_i^c(c,d)}{\partial d}\right]^2 \tag{5}$$

We can see that the sensitivity coefficients are introduced to express the gradients and the Hessian matrix defined in equations (4) and (5).

$$\chi_{ij}=\frac{\partial H_i^c(c,d)}{\partial j},\ i=1,\ldots N \text{ and } j=c \text{ or } d \tag{6}$$

The sensitivity coefficient χ_{ij} means the change of thicknesses H_i^c caused by the variation of the parameters *c* and *d*. Due to the nonlinearity of the model, an explicit expression of the sensitivity coefficient cannot be obtained. Instead, a numerical scheme should be used. In the present study, a central finite difference scheme is employed to evaluate the above derivative.

$$\frac{\partial H_i^c(c,d)}{\partial c} = \frac{H_i^c(c+\varepsilon,d) - H_i^c(c-\varepsilon,d)}{2\varepsilon} \text{ and } \frac{\partial H_i^c(c,d)}{\partial d} = \frac{H_i^c(c,d-\varepsilon) - H_i^c(c,d-\varepsilon)}{2\varepsilon} \quad (7)$$

where ε is a small number.

Levenberg-Marquardt Method

The current optimization problem is solved by the Levenberg-Marquardt method [18]. This method assumes the advantages of the steepest descent method and the inverse-Hessian method, while it covers the disadvantages of both methods. Hence, it has become the standard of nonlinear least-square routines. In this approach, the Hessian matrix is newly defined.

$$\alpha_{cc}^{'} = \alpha_{cc}(1+\lambda),\ \alpha_{dd}^{'} = \alpha_{dd}(1+\lambda) \text{ and } \alpha_{cd}^{'} = \alpha_{cd} \quad (8)$$

Then, the parameters c and d are obtained iteratively, following the recommended Marquardt recipe for an initial guess of c and d. If a value of $S(c,d)$ stops decreasing practically, the iteration is terminated and the corresponding parameters c and d are the compressibility coefficients obtained.

Results

The inverse method is applied to the experimental hydro-mechanical curves (Fig. 2). The measured thickness and the computed thickness with the compressibility obtained by the inverse search are compared in Fig. 3.

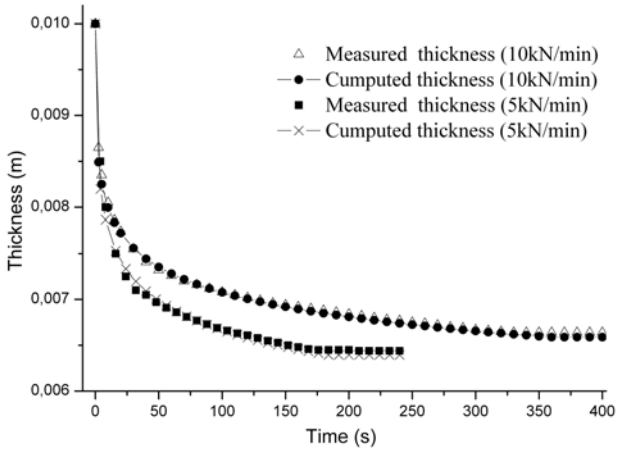

Fig. 3 Comparison of measured thickness and computed thickness.

A good agreement is observed between the computed thickness obtained by the compressibility parameters in Table 1 and the measured thickness obtained by experimental hydro-mechanical loading. The compressibility curves obtained from the inverse method modelling (parameters given in Table 1) are compared to experimental curves determined with imposed compression velocities (between 0.25 to 2 mm/min) in Fig. 4. This figure shows that the stresses required to compacting fibrous preforms saturated by the fluid rise with an increasing compaction speed as

already mentioned by Robitaille and Gauvin [10] for dry compression of satin glass weave. This is due to the viscoelastic behaviour of the preform studied.

Table 1 Compressibility parameters

	First parameter c	Second parameter d
Load (5 kN/min)	$8{,}73\, e^{8}$	17,49
Load (10kN/min)	$2{,}24\, e^{8}$	14,45

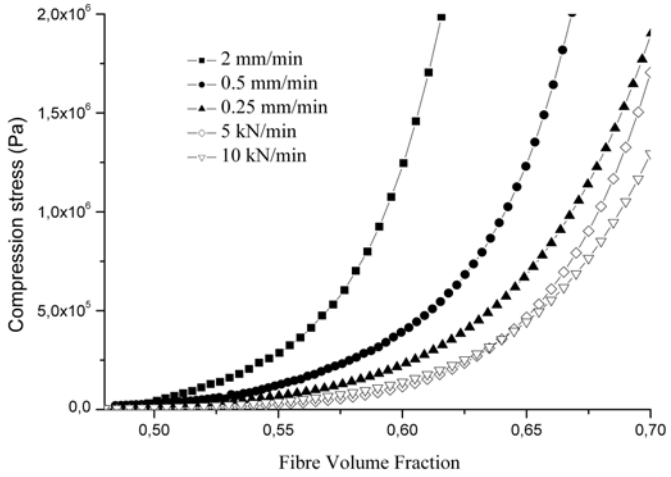

Fig. 4 Comparison of experimental and numerical compressibility curves.

CONCLUSIONS

A hydro-mechanical coupling code developed for simulation of infusion processes is used with an inverse method to predict the compressibility behaviour of the fibrous preform. An experimental device developed at Le Havre is used to apply hydro-mechanical loads to the reinforcements. Two ramps of stress are imposed to the preform and the change of the thickness is measured as a function of time. The measured thickness and the computed thickness with the compressibility obtained by the inverse method are compared, and a good agreement is observed.

REFERENCES

1. J. Park and M. K. Kang. A Numerical Simulation of the Resin Film Infusion Process. *Composite Structures*, 2003; 60(4): 431–437.

2. V. Antonucci, M. Giordano, L. Nicolais, A. Calabrò, A. Cusano and A. Culoto. Resin Flow Monitoring in the Resin Film Infusion Process. *J Mater Process Technol.* 2003; 143–144:687–92.

3. I. Sevotianov, V. E. Verijenko and C. J. Klemperer. Mathematical Model of Cavitation During Resin Film Infusion Process. *Composite Structures,* 2000; 48:197–203.

4. N. L. Han, S. S. Suh, J. M. Yang and H. T. Hahn. Resin Film Infusion of Stitched Stiffened Composite Panels. *Composites Part A: Applied Science and Manufacturing,* Volume 34, pages 227-236 (2003).

5. J. L. Sommer and A. Mortensen. Forced Unidirectional Infiltration of Deformable Porous Media. *J Fluid Mech*, 1996;22:1205–22.

6. D. Ambrosi and L. Preziosi. Modelling Matrix Injection Through Elastic Porous Preforms. *Composites Part A: Applied Science and Manufacturing,* Volume 29, pages 5-18 (1998).

7. S. Lopatnikov, P. Simacek, J. Gillespie and S. G. Advani. A Closed form Solution to Describe Infusion of Resin Under Vacuum in Deformable Fibrous Porous Media. *Model Simul Mater Sci Eng* 2004;12:191–204.

8. T. Ouahbi, A. Saouab, J. Breard, P. Ouagne and S. Chatel. Modelling of Hydro-Mechanical Coupling in Infusion Processes. *Composites Part A, Applied Science and Manufacturing*. Volume: 38, Issue 7, July 2007, pp.:646-1654.

9. T. G. Gutowski and G. Dillon. The Elastic Deformation of Fiber Bundles. In: Gutowski TG, editor. *Advanced composites manufacturing*. Willey; 1997, p. 138–9.

10. F. Robitaille and R. Gauvin. Compaction of Textile Reinforcements for Composite Manufacturing. I. Review of Experimental Results. *Polymer Composites*, 1998;19(2):198–216.

11. Y. Luo and I. Verpoest. Compressibility and Relaxation of a New Sandwich Textile Preform for liquid Composite Molding. *Polymer Composites*, 1999; 20(2):179–91.

12. R. A. Saunders, C. Lekakou and M. G. Bader. Compression in the Processing of Polymer Composites 1. A Mechanical and Microstructural Study for Different Glass Fabrics and Resins. *Composites Science and Technology*, 1999;59: 983–93.

13. Y.R. Kim, S.P. Mc Carthy and J.P, Fanucci. Compressibility and Relaxation of Fiber Reinforcements During Composite Processing. *Polymer Composites*, 1991, vol. 12, p. 13-19.

14. S. Toll and J. A. E. Manson. An Analysis of the Compressibility of Fiber Assemblies. In: *Proceeding of the sixth International Conference on Fiber-Reinforced Composites*, Institute of Materials, Newcastle upon Tyne, UK, 1994, p. 25/1–25/10.

15. D. Mehri, V. Michaud, E. Comte and J. A. E. Manson. Predicting the Sizing Dependent Rigidity of Glass Fibre Bundles in Sheet Moulding Compounds. *Composites Part A: Applied Science and Manufacturing,* 37 (2006) 1773-1786.

16. S. Cadinot. Aspects rhéologiques de la compressibilité d'un renfort fibreux pour matériaux composites: études en compression et relaxation. *These de Doctorat* 2002. Université du Havre.

17. P. A. Kelly, R. Umer and S. Bickerton. Viscoelastic Response of Dry and Wet Fibrous Materials During Infusion Processes. *Composites Part A: Applied Science and Manufacturing,* 2006; 37: 868–73.

18. Press W.H., Teukolsky S.A., Vetterling W.T. and Flannery B.P., "*Numerical recipes"*. 2nd edition, Cambridge university press, 1992.